Animal Nutrition 19 (2024) 248–260

Contents lists available at ScienceDirect

Animal Nutrition

journal homepage: http://www.keaipublishing.com/en/journals/aninu/

Original Research Article

Evaluation of glycyrrhetinic acid in attenuating adverse effects of a high-fat diet in largemouth bass (*Micropterus salmoides*)

Quanquan Cao [†], Zhihao Zhang [†], Ju Zhao, Lin Feng, Weidan Jiang, Pei Wu, Juan Zhao, Haifeng Liu [*], Jun Jiang [*]

College of Animal Science and Technology, Animal Nutrition Institute, Sichuan Agricultural University, Chengdu 611130, China

ARTICLE INFO

Article history:
Received 28 July 2023
Received in revised form
12 April 2024
Accepted 19 September 2024
Available online 23 September 2024

Keywords:
Glycyrrhetinic acid
Pyroptosis
Inflammation
Intestine
Largemouth bass

ABSTRACT

Glycyrrhetinic acid (GA) has been shown to promote growth characteristics and play a crucial role in anti-inflammatory responses in animals. To investigate the effects of dietary GA supplementation on growth performance, intestinal inflammation, and intestinal barrier protection in largemouth bass (*Micropterus salmoides*) fed a high-fat diet (HFD), a 77-day feeding experiment was conducted. A total of 750 largemouth bass, initially averaging 17.39 ± 0.09 g in body weight, were randomly allocated to five experimental groups and fed a control diet, a HFD, and the HFD diet supplemented with GA at either 0.5, 1.0, or 1.5 mg/kg, named as control, HDF, HFD + GA 0.5, HFD + GA 1.0, and 1.5 HFD + GA 1.5, respectively. Each group contained three replicates. The study revealed that dietary GA improved final body weight ($P < 0.001$), percent weight gain ($P = 0.041$), and feed intake ($P < 0.001$), all of which had been affected by a HFD in largemouth bass ($P < 0.05$). Supplementation of HFD with 1.0 mg/kg GA increased the mRNA expressions and protein levels of corresponding tight junctions, occludin, zonula occluden-1 (ZO-1) and claudin-1 in the intestines of largemouth bass. Furthermore, the addition of HFD with both of 0.5 and 1.0 mg/kg GA decreased the mRNA expressions of pro-inflammatory genes such as interleukin-1β (*IL-1β*), *IL-18*, and cysteinyl aspartate specific proteinase 1 (*caspase-1*), as well as proteins associated with pyroptosis-induced inflammation, including NOD-like receptor family and pyrin domain contain 3 (NLRP3), apoptosis-associated speck-like protein containing a C-terminal caspase recruitment domain (ASC), gasdermin E (GSDME), and N-terminal domain of GSDME (GSDME-N) ($P < 0.05$). Finally, dietary GA supplementation alleviated mitochondrial damage and reduced reactive oxygen species (ROS) production induced by the HFD. It is concluded that GA supplementation in HFD enhances growth performance, increases mRNA expression and protein levels of tight junction-related parameters, decreases mRNA expression and protein levels of pyroptosis-related genes, and alleviates intestinal mitochondrial injury and inflammation induced by HFD.

1. Introduction

Largemouth bass (*Micropterus salmoides*) is a widely farmed freshwater fish in China due to its rapid growth, delectable meat, and significant market value. This fish species is widely favored in commercial production (Chen et al., 2021; Yuan et al., 2019). Being a carnivorous species, protein is the costliest nutrient in their feed. Protein levels in their diet significantly influence the growth performance of these fish (Bahnasa, 2009). Lipids are cost-effective source of energy compared to protein, and are frequently employed in aquatic animal feeds because of their ability to conserve protein. Adding sufficient lipids to diets can effectively save protein consumption, commonly known as the "protein

*Corresponding authors.
E-mail addresses: liuhf@sicau.edu.cn (H. Liu), jjun@sicau.edu.cn (J. Jiang).
[†] These two authors contributed equally to this manuscript.
Peer review under the responsibility of Chinese Association of Animal Science and Veterinary Medicine.

Production and Hosting by Elsevier on behalf of KeAi

https://doi.org/10.1016/j.aninu.2024.09.002

sparing" effect (Hillestad et al., 1994). Recently, the aquaculture industry has explored the use of high-fat diets (HFD) as a means to reduce feed cost and minimize resource wastage (Sagada et al., 2017; Wang et al., 2019). However, HFD reduce the percent weight gain (PWG) and specific growth rate (SGR) of largemouth bass (Chen et al., 2023). Prolonged feeding of HFD to fish can result in an excessive buildup of lipids in their internal organs and tissues (Guo et al., 2019; Yin et al., 2021; Zhang et al., 2020). This excess lipid accumulation can lead to the production of reactive oxygen species (ROS) and worsen inflammation, ultimately affecting fish growth performance and health (Chatzifotis et al., 2010; Morais et al., 2001; Wang et al., 2005).

It is important to note that pyroptosis, which differs significantly from necroptosis and apoptosis, is a distinct form of programmed cell characterized by cell swelling, cell membrane rupture, cell lysis, and a pronounced pro-inflammatory response (Wu et al., 2021). Some studies have demonstrated that pyroptosis can result in the formation of pores in the cell membrane, compromising the integrity of the intestinal barrier (Liu et al., 2021; Zhou and Fang, 2019). In response to toxin treatment or pathogen infection, multiple inflammasome complexes are formed, leading to the activation of various cysteinyl aspartate specific proteinases (caspases), including caspase-1, -4, -5, -11, and −12 (Shi et al., 2015). In mammals, the typical pyroptosis pathway results in the creation of cell membrane pores, allowing ion exchange, under the influence of caspase-1 and the activation of gasdermin-E (GSDME) (Gaul et al., 2021). Meanwhile, the maturation of interleukin-1β (IL-1β) and interleukin-18 (IL-18) is initiated by cleaved caspase-1, ultimately leading to pyroptosis (Wei et al., 2019). However, recent research has revealed that the fish genome lacks GSDMD and that GSDME functions in fish similarly to mammals, both playing pivotal roles in pyroptosis (Li et al., 2020; Wang et al., 2022). In mammals, NOD-like receptor (NLR) family pyrin domain-containing (NLRP) 1, NLRP3, NLRP12, and NLR family caspase activation and recruitment domain-containing 4 (NLRC4) are key sensory molecules in inflammasomes (Franchi et al., 2009; Zhang et al., 2021). Moreover, in teleosts, NLRP1 and NLRP3 from zebrafish and NLRP3 from the Japan flounder were identified only as inflammasome-forming NLRs (Li et al., 2018, 2020). Among all vertebrates, with the exception of cyprinid fish, pro-caspase-1 is self-proteolyzed into the active-form caspase-1 after binding with pyridinoline and a C-terminal caspase-recruitment domain (ASC) containing apoptosis-associated speck-like protein, mutually catalyzing other pro-caspase-1 (Kersse et al., 2011; Srinivasula et al., 2002). A recent study has highlighted the critical role of NLRP3-related pyroptosis in intestinal diseases, particularly those induced by a HFD intake (Zhang et al., 2021). However, published literature on the mechanism of pyroptosis in fish-related intestinal injuries is lacking.

High mobility group box 1 (HMGB1) is abundantly expressed in various cell nuclei and plays a significant role in gene transcription across various diseases (Sims et al., 2010). HMGB1 is a widely distributed, non-sequence-specific nuclear transcription factor in eukaryotic cells that binds to DNA in a minor groove. Numerous studies have demonstrated the significant role of HMGB1 in transcription, DNA integration, and modulation (Yamada, 2004). It is well-established that HMGB1 release in mammals is an active process regulated by ROS (Han et al., 2015; Li et al., 2019; Min et al., 2017; Tsung et al., 2007). HMGB1 is considered to be a typical damage-associated molecular pattern (DAMP) molecule. It can cause cell death and tissue damage by acting on receptors (Bianchi et al., 2017). Passive release and active release are the two main pathways of HMGB1 release (Li et al., 2019). The involvement of HMGB1 in the inflammatory process is mediated through receptor for advanced glycation end-products (RAGE). Ultimately, this binding activates the NLRP3 cascade response and triggers the production of relevant pro-inflammatory cytokines (Arab et al., 2021; Geng et al., 2015). RAGE binds HMGB1 to the lysosomes and induces the activation and release of pepsin B from the lysosomes, and activation of the NLRP3 inflammasome by binding to NLRs (Jia et al., 2019). These findings suggest that HMGB1 regulates inflammation caused by NLRP3.

Glycyrrhetinic acid (GA) is a pentacyclic triterpene derivative obtained from the hydrolysis of β-amyrin-type licorice (Roman Paduch, 2014). It stands out as the most significant bioactive component of licorice root, exerting a wide range of biological activities, including anti-inflammatory, antiviral, anti-oxidative, and anti-cancer effects (Fiore et al., 2008; Han et al., 2015). Several studies have demonstrated that the triterpene structure of GA can bind to HMGB1, thereby altering the pro-inflammatory properties of the protein (Mollica et al., 2007; Yamaguchi et al., 2012). These findings suggest that GA can reduce the production of ROS (Cai et al., 2018). The objectives of our study were to investigate the effects of dietary GA on growth performance and the alleviating effect on largemouth bass intestinal injury under HFD.

2. Materials and methods

2.1. Animal ethics statement

This animal experiment complied with the ARRIVE guidelines (https://arriveguidelines.org/). The study was conducted in strict compliance with the Experimental and Ethics Animal Committee of Sichuan Agricultural University, Ya'an, China (Permit No. DKY-S20210416).

2.2. Experimental diets

Table 1 presents the feed formulation and nutritional composition of the experimental diets. The dietary protein sources included fish meal, chicken powder, gluten meal and fermented soybean meal, with soybean oil serving as a lipid source. Fish were divided into five groups as follows: control (48.23 % crude protein, 9.05 % crude lipid); HFD (46.50 % crude protein, 16.29 % crude lipid); HFD supplemented with GA at 0.5 mg/kg (HFD + GA 0.5; 47.48 % crude protein, 16.25 % crude lipid); HFD supplemented with GA at 1.0 mg/kg (HFD + GA 1.0; 47.48 % crude protein, 16.44 % crude lipid); HFD supplemented with GA at 1.5 mg/kg (HFD + GA 1.5; 47.55 % crude protein, 16.44 % crude lipid) for 77 d. All dry ingredients were crushed in a mill. Diets were processed into puffed feed using a machine (TPE62S, Tianjin Plastic Extruder Co., Ltd., China) and a vacuum coater (KDVM1, KERUNDE, China). The floating extruded pellets were air-dried and stored at 4 °C in plastic bags until being used.

2.3. Fish management and feeding

A total of 750 Largemouth bass fish with an average weight of 17.39 ± 0.09 g were obtained from the New Hope Feed Research and Development base in Sichuan, China. Fish were allowed to acclimate to their environment for two weeks before the commencement of the experiment. Fifteen concrete tanks (200 cm × 100 cm × 105 cm) were used, housing 50 fish in each experimental tank. Each group contained three replicates. The fish were manually fed twice a day (07:30 and 18:00) for 77 d under natural photoperiod condition, ensuring they reached a satiated state with each feeding. Any uneaten feed was collected 30 min after each feeding session and subsequently dried in an oven at 65 °C to determine the feed intake (FI). Initial body weight (IBW) and Final body weight (FBW) were measured and survival rate (SR), percent weight gain (PWG), specific growth rate (SGR) and feeding efficiency (FE) were calculated.

Table 1
Formulation and proximate composition of the experimental diets (% dry matter).[1,2].

Item	Control	HFD	HFD + GA 0.5	HFD + GA 1.0	HFD + GA 1.5
Ingredients					
Soybean oil	6.00	12.00	12.00	12.00	12.00
Bentonite	7.00	1.00	0.00	0.00	0.00
Fish meal	43.00	43.00	43.00	43.00	43.00
Chicken powder	16.00	16.00	16.00	16.00	16.00
Gluten meal	7.00	7.00	7.00	7.00	7.00
Fermented soybean meal	5.00	5.00	5.00	5.00	5.00
Whole meal flour	6.00	6.00	6.00	6.00	6.00
Cassava starch	5.70	5.70	5.70	5.70	5.70
Lysine	0.20	0.20	0.20	0.20	0.20
Methionine	0.20	0.20	0.20	0.20	0.20
Calcium biphosphate	1.00	1.00	1.00	1.00	1.00
GA Premix	0.00	0.00	1.00	1.00	1.00
Choline chloride	0.40	0.40	0.40	0.40	0.40
Premix[3]	2.50	2.50	2.50	2.50	2.50
Nutrient levels[4]					
Crude protein	48.23	46.50	47.48	47.48	47.55
Crude lipid	9.05	16.29	16.25	16.44	16.44
Crude ash	11.64	11.88	11.69	11.52	11.40
Moisture	5.61	5.52	5.60	5.49	5.50

[1] Fish were fed five different diets, including control diet, high fat diet (HFD), and HFD, diet supplemented with glycyrrhetinic acid (GA) at 0.5, 1.0, or 1.5 mg/kg for 11 weeks.
[2] Glycyrrhetinic acid premix (Jiang Xi Revere Biotechnology Co., Ltd., China) was mixed with bentonite.
[3] Premix contain the following minerals (mg/kg premix) and vitamins (mg/kg premix): $FeSO_4•H_2O$, 100.00; $MgSO_4•H_2O$, 625.00; $CuSO_4•5H2O$, 20; $ZnSO_4•H_2O$, 115.94; $MnSO_4•H_2O$, 37.74; $CoCl_2•6H_2O$, 81.97; $Ca(IO_3)_2$, 61.35; Na_2SeO_3, 200; KCl, 95.60; NaCl, 76.26, vitamin A, 133.33; vitamin E, 220.00; vitamin B_{12}, 100.00; vitamin D_3, 2.40; folic acid, 2.00; biotin, 50.00; Inositol, 408.16; vitamin B_1, 21.00; vitamin B_2, 43.75; vitamin B_6, 22.00; vitamin K_3, 23.23; acid regurgitation, 37.76; vitamin C, 157.89.
[4] Crude protein, crude lipid, moisture, and crude ash were measured values.

After the culture experiment, the fish were anesthetized with a tricaine methanesulfonate (MS-222; 1 %, Sigma, USA) solution after a 24-h fasting period. The total number and weight of the fish were measured and recorded after they were removed from each tank. Three fish were selected randomly from each tank and stored at −20 °C to determine their body composition. The fish were immediately dissected using a sterile scalpel, and intestinal samples were taken. Twelve fish from each tank were removed, frozen in liquid nitrogen, and stored at −80 °C for later RNA extraction and Western blot analysis.

2.4. Biochemical analysis

The dry matter content of the diets and fish were analyzed according to the method 934.01 (AOAC, 1990). The samples were desiccated at a temperature of 104 °C until constant weight for the analysis of dry matter. The total nitrogen (N) was determined according to the method 968.0 (AOAC, 1990) after acid digestion was performed. The crude protein (CP) was obtained by multiplying the total N content by 6.25. The moisture was determined according to the method 935.29 (AOAC, 1990). The crude lipid (EE) was analyzed using the Soxhlet extraction method 983.15 (AOAC, 1990), and the ash contents were examined in the muffle furnace at 550 °C for 4 h according to the method 942.05 (AOAC, 1990).

2.5. Histological analysis

After thorough rinsing of tissues in 70 % ethanol, the samples were dehydrated in a graded ethanol series and embedded in Paraplast (Leica Microsystem, Wetzlar, Germany). Transverse sections (5 μm) were cut using a microtome (Typ 1400; Leitz, Wetzlar, Germany), collected on poly-L-lysine-coated glass slides, and stained using the hematoxylin-eosin (H&E) staining protocol (Buzete et al., 2019). The slides were observed under a microscope (DIAPLAN; Ernst Leitz GmbH, Wetzlar, Germany), and the kidney sections were photographed.

2.6. Transmission electron microscopy

The intestines were sliced into approximately 1 mm thickness and fixed in 3% glutaraldehyde in pH 7.4 cacodylate buffer for 24 h at room temperature. Then the intestines were washed three times in phosphate-buffered saline (PBS) and soaked in 1 % osmic acid for 1.5 h. The samples were dehydrated in resin. Cross-oriented ultrathin sections were sliced into ultrathin sections using an ultramicrotome and images were acquired on a transmission electron microscope (HT7800, Hitachi High-Tech Corporation, Japan) (De et al., 1991).

2.7. Biochemical index assays

Malonic dialdehyde (MDA) is a crucial byproduct of membrane lipid peroxidation, and its production can exacerbate membrane damage. Adenosine triphosphate (ATP) indicates mitochondrial damage, while lactate dehydrogenase (LDH) indicates the extent of cell damage. The activities of MDA, ATP and LDH were tested using a commercial kit (Nanjing Jiancheng Corporation, China) according to the manufacturer's instructions.

2.8. Fluorescence staining assay

A ROS assay was used to determine ROS accumulation in the intestinal cell suspension. Cells were stained with 4′,6-diamidino-2′-phenylindole (DAPI) and co-cultured with 2,7-dichlorodihydrofluorescein diacetate (DCFH-DA) (ThermoFisher, USA) for 30 min at 37 °C. The levels of ROS accumulation were detected using a fluorescence spectrophotometer and a light microscope (BX53, Olympus, Japan).

A commercial assay kit with a lipophilic cation JC-1 probe (Beyotime Institute of Biotechnology, Haimen, China) was used to detect changes in mitochondrial membrane potential. As per the manufacturer's instructions, a cell suspension was prepared from intestinal tissue. The treated cells were incubated with 1 mL JC-1 staining working solution for 30 min at 37 °C and washed twice using JC-1 staining buffer. Finally, red and green fluorescence was

determined using a light microscope (BX53, Olympus, Japan) and a fluorescence spectrophotometer.

2.9. Real-time quantitative PCR

RNA was extracted from the intestine using the RNAiso Plus Kit (TaKaRa, Dalian, Liaoning, China), followed by DNase I treatment. The RNA's integrity and purity were assessed by spectrophotometric (the ratio of the absorbance values of 260 nm vs 280 nm) analysis and agarose gel (1%) electrophoresis. The total RNA concentration was diluted to 500 ng/μL, and reverse transcription was performed using the Prime Script RT reagent kit with gDNA Eraser (Vazyme, Nanjing, Jiangsu, China). Specific primers of genes were designed based on published sequences of largemouth bass (Table 2). Real-time PCR detection was performed in a CFX96 Real-Time PCR Detection System (Bio-Rad, Hercules, CA, USA). The concentration of the target gene's mRNA was normalized to the mRNA concentration of the reference genes β-actin and *18S* rRNA. The following program included a denaturation step at 95 °C for 1 min, followed by 40 amplification cycles of 5 s of denaturation at 95 °C, 15 s of annealing at 60 °C, and 20 s of extension at 72 °C. A melt-curve analysis was performed, followed by storage at 4 °C. The results were calculated using the $2^{-\Delta\Delta Ct}$ method after verification. The 18 S and β-Actin were referred as reference genes.

2.10. Western blot analysis

The protein levels of the pyroptosis pathway and tight junction-related genes were assessed following a previously established protocol (Huo et al., 2021). The BCA kit (Beyotime, China) was used to calculate protein concentrations according to the manufacturer's instructions. Equal amounts of proteins (20 μg) were subjected to SDS-PAGE gel and transferred onto a polyvinylidene difluoride (PVDF) membrane. After blocking in 5% nonfat milk powder for 1.5 h, the membranes were incubated with primary antibodies, including anti-β-actin (dilution 1:5000, ABclonal, China), anti-HMGB1 (dilution 1:1000, ABclonal, China), anti-RAGE (dilution 1:1000, ABclonal, China), anti-NLRP3 (dilution 1:1000, ABclonal, China), anti-ASC (dilution 1:1500, ABclonal, China), anti-GSDME (dilution 1:3500, ABclonal, China), anti-IL-1β (dilution 1:1000, ABclonal, China), anti-ZO-1 (dilution 1:1000, ABclonal, China), anti-occludin (dilution 1:1000, ABclonal, China), and anti-claudin-1 (dilution 1:1000, ABclonal, China) overnight at 4 °C with shaking. The membranes were then washed five times (5 min/wash) with 1 × TBST, and the anti-rabbit IgG-HRP (1:2000) was added. The membranes were incubated for 1.5 h with shaking and then washed five times (5 min/wash) with 1 × TBST. The protein bands were visualized using ECL reagents (Beyotime, China), and the protein content was assessed using Image-J software.

2.11. Immunohistochemistry

For immunohistochemistry of HMGB1, ZO-1, and caspase-1, sections were dewaxed (Histochoice Clearing Agent, Sigma−Aldrich), hydrated through a descending series of ethanol baths (from 100% to 50%), and rinsed in PBS (pH 7.4; Bio-Rad Laboratories, USA). Slides were then immersed for 10 min in 0.02 % Tween 20 and 150 mmol/L NaCl in PBS, pH 7.3. After incubation in 5 % bovine serum albumin (BSA) in PBS for 20 min, the slides were rinsed three times with PBS. Primary labeling was performed for 2 h at room temperature in a humidity chamber placed on a shaker using the following antibodies: mouse monoclonal antibody raised against rabbit anti-HMGB1, ZO-1 in 0.5% BSA in PBS. Control slides without the primary antibodies were also prepared. After three washes in PBS to remove unbound antibody, the sections were incubated for 1 h with a secondary antibody at 10 μg/mL (goat anti-mouse Alexa Fluor 594, Invitrogen Life Technologies, Switzerland, and donkey anti-rabbit Alexa Fluor 488, Thermo Fisher Scientific, USA).

After washing, nuclei were counterstained with DAPI for 2 min, and the sections were thoroughly washed in PBS. They were then mounted in an anti-bleaching mounting medium (Immunohistomount, Santa Cruz Biotechnology, USA) for observation using a Leica DM6B microscope (DIAPLAN; Ernst Leitz GmbH, Wetzlar, Germany) equipped with a special filter set for fluorescence and coupled to a Leica DMC 2900 digital camera (DIAPLAN; Ernst Leitz GmbH, Wetzlar, Germany). Posterior kidney sections were photographed using objectives with magnifications of 4× and 10× .

2.12. Statistical analysis

The data were analyzed using the PROC MIXED procedure of SAS 9.3 (SAS Inst. Inc., Cary, NC, USA) using the model:

$$Y_{ijkl} = \mu + T_i + P_j + S_k + C(_k)_l + T \times S_{ik} + e_{ijkl},$$

where Y_{ijkl} refers to the dependent variable; μ, the overall mean; T_i, the fixed treatment effect; P_j, the random period effect; S_k, the random square effect; $C(_k)_l$, the random effect of the lth steer within the kth square; $T \times S_{ik}$, the interaction between the $_i$th treatment and the kth square; and e_{ijkl}, the error residual. The linear and quadratic effects of increasing levels of GA were evaluated using the CONTRAST procedure of SAS 9.3. The Kenward-Roger option was

Table 2
Primer sequences of genes selected for qPCR.

Item	Sequence (5′ to 3′)	Product size, bp	Accession number
Caspase-1	F: CCTTGTCTGCTCTGCTGCTATTC R: GGGTGAGGAGTAAGTTTGTGGA	138	XM_038694367.1
IL-1β	F: TGGACAGAACAACGGGACTACT R: CGACCGCAGTAAGAAAGACATC	161	XM_038733429.1
IL-18	F: GGTAAGTGTCCTCATCCCAATCTG R: GGAACTGTCCACCGCATCTC	146	XM_038692744.1
ZO-1	F: ATCTCAGCAGGGATTCGACG R: CTTTTGCGGTGGCGTTGG	208	XM_038706143.1
Occludin	F: TGGGTAGGCGTTGTAATCACTC R: CTACAGTCCTCCTTTCACCTCG	91	XM_038715418.1
Cludin1	F: GCCATTTGTAGAAGTGCTGCG R: GTCTACAGTCCTCCTTTCACCTCG	148	XM_038718401.1
β-Actin	F: CCCCATCCACCATGAAGA R: CCTGCTTGCTGATCCACAT	120	AF253319.1
18S	F: TGAATACCGCAGCTAGGAATAATG R: CCTCCGACTTTCGTTCTTGATT	201	MH018569.1

Caspase-1 =cysteinyl aspartate specific proteinase 1; *IL* = interleukin; *ZO* = zonula occludens, *18S* = 18 ribosomal RNA.

Table 3
Growth performance of *Micropterus salmoides* fed diets with graded glycyrrhetinic acid (GA) levels [1].

Item	Dietary GA levels					SEM	*P*-value		
	Control	HFD	HFD+GA 0.5	HFD+GA 1.0	HFD+GA 1.5		ANOVA	Linear	Quadratic
IBW, g/fish	17.60	17.44	17.41	17.31	17.35	0.557	0.926	0.985	0.533
FBW, g/fish	102.48^{ab}	95.66^{a}	111.42^{b}	108.50^{b}	96.93^{a}	2.069	<0.001	0.032	<0.001
SR[2], %	99.33	98.67	100.00	98.00	98.00	0.008	0.627	0.331	0.703
PWG[3], %	480.93^{b}	448.47^{a}	542.01^{c}	526.79^{c}	458.52^{a}	21.791	0.041	0.200	0.023
SGR[4], %/d	2.28^{a}	2.20^{a}	2.41^{b}	2.38^{b}	2.23^{a}	0.049	0.049	0.212	0.025
FI[5], g/fish	81.29^{ab}	74.74^{a}	82.15^{ab}	84.88^{b}	79.23^{ab}	1.265	<0.001	0.044	<0.001
FE[6], %	104.99^{a}	105.71^{a}	115.08^{b}	107.09^{a}	100.73^{a}	2.106	0.002	<0.001	0.097

HFD = high fat diet; IBW = initial body weight; FBW = final body weight; SR = survival rate; PWG = percent weight gain; SGR = specific growth rate; FI = feed intake; FE = feed efficiency.
[a, b, c] Different superscript letters within a row indicate significant differences ($P < 0.05$).
[1] HFD+GA 0.5, HFD diet supplemented with 0.5 mg/kg GA; HFD+GA 1.0, HFD diet supplemented with 1.0 mg/kg GA; HFD+GA 1.5, HFD diet supplemented with 1.5 mg/kg GA. Values are mean ± SE of three replicate groups, while quadratic regression was run with the triplicate data points.
[2] Survival rate (%) = 100 × final number of fish/initial number of fish.
[3] Percent weight gain (%) = 100 × (FBW - IBW)/IBW.
[4] SSpecific growth rate (%/d) = 100 × (ln FBW - ln IBW)/days.
[5] Feed intake (g/fish) = (feed offered as DM basis - uneaten feed as DM basis)/number of fish.
[6] Feed efficiency (%) = 100 × (FBW - IBW)/FI.

used to calculate the degrees of freedom. Differences among the means of different treatments were tested using Duncan's test. Effects were considered significant at $P < 0.05$. All values are presented as least squares means ± standard errors (SE).

3. Result

3.1. Growth performance and somatic parameters

Growth performance in Largemouth bass was evaluated after 11 weeks of feeding trial (Table 3). The results indicated that the final body weight (FBW), percent weight gain (PWG), specific growth rate (SGR), and FI of the HFD + GA 0.5 and HFD + GA 1.0 groups were higher than those of the HFD and HFD + GA 1.5 groups ($P < 0.05$). The HFD + GA 0.5 group exhibited the highest feed efficiency (FE) compared to the other groups while the control and HFD + GA 1.5 groups had the lowest ($P = 0.002$). Survival rates (SR) did not show significant differences between any of the groups.

As presented in Table 4, viscera weight (VW) was considerably affected by the HFD and the addition of 0.5 and 1.0 mg/kg GA groups ($P < 0.001$). The groups fed the HFD, HFD + GA 0.5, and HFD + GA 1.0 diets displayed higher values than the NC and HFD + GA 1.5 groups. The visceral somatic index (VSI) was highest in the HFD group compared to the other groups ($P < 0.001$). Compared to the control group, HFD group fish had higher intestinal weight (IW). However, fish morphology was not affected by the addition of GA to the feed. There were no significant differences in somatic index (ISI), intestinal length (IL), or relative gut length (RGL) among the groups.

3.2. Whole body proximate composition

Table 5 displays the results of whole-body composition of fish. The moisture and lipid content had no difference among the groups. Diets with different GA additions had no effect on the crude protein and crude ash content of fish. HFD + GA 0.5 group showed a higher ash production value (APV) value than the HFD + GA 1.5 group ($P = 0.008$). The protein production value (PPV) exhibited a similar expression trend to the APV ($P = 0.049$). Compared to the

Table 4
Biometric parameters of *Micropterus salmoides* fed diets with graded glycyrrhetinic acid (GA) levels [1].

Item	Dietary GA levels					SEM	*P* value		
	Control	HFD	HFD+GA 0.5	HFD+GA 1.0	HFD+GA 1.5		ANOVA	Linear	Quadratic
VW, g/fish	9.10^{a}	11.39^{b}	10.77^{b}	10.85^{b}	9.72^{a}	0.348	<0.001	0.113	0.877
VSI[2], %	8.94^{a}	11.07^{c}	10.01^{b}	9.66^{ab}	10.06^{b}	2.069	<0.001	0.032	<0.001
LW, g/fish	2.46	3.10	3.39	3.39	3.37	0.008	0.627	0.331	0.703
HSI[3], %	2.44^{a}	3.01^{b}	3.14^{b}	3.01^{b}	3.48^{c}	21.791	0.041	0.200	0.023
IW, g/fish	0.70^{a}	0.73^{a}	0.78^{a}	0.84^{b}	0.76^{a}	0.049	0.049	0.212	0.025
ISI[4], %	0.69^{a}	0.72^{ab}	0.72^{ab}	0.74^{ab}	0.78^{b}	0.165	<0.001	0.044	<0.001
IL, cm/fish	11.90^{a}	12.47^{ab}	12.75^{b}	12.27^{ab}	11.67^{a}	2.106	0.002	<0.001	0.097
RGL[5], %	71.98^{a}	76.04^{b}	76.50^{b}	71.47^{a}	70.38^{a}	1.716	0.041	0.012	0.764

HFD = high fat diet; VW = viscera weight; VSI = viscerosomatic index; LW = liver weight; HSI = Hepatosomatic index; IW = intestinal weight; ISI = intestosomatic index; IL = intestinal length; RGL = relative gut length.
[a, b, c] Different superscript letters within a row indicate significant differences ($P < 0.05$).
[1] HFD+GA 0.5, HFD diet supplemented with 0.5 mg/kg GA; HFD+GA 1.0, HFD diet supplemented with 1.0 mg/kg GA; HFD+GA 1.5, HFD diet supplemented with 1.5 mg/kg GA. Values are mean ± SE of three replicate groups, with 6 fish per tank.
[2] Viscerosomatic index (%) = 100 × wet viscera weight/wet body weight.
[3] Hepatosomatic index (%) = 100 × wet liver weight/wet body weight.
[4] Intestosomatic index (%) = 100 × wet intestine weight/wet body weight.
[5] Relative gut length (%) = 100 × intestine length/body length.

Table 5
Whole-body (wet-weight basis) of *Micropterus salmoides* fed diets with graded glycyrrhetinic acid (GA) levels (%)[1].

Item	Dietary GA levels					SEM	*P*-value		
	Control	HFD	HFD+GA 0.5	HFD+GA 1.0	HFD+ GA 1.5		ANOVA	Linear	Quadratic
Moisture	69.28	68.04	67.92	68.41	68.28	0.214	0.376	0.271	0.631
Protein	19.31	19.31	19.56	19.60	19.25	0.184	0.445	0.651	0.125
Lipid	7.40	8.52	8.25	8.01	8.16	0.134	0.085	0.079	0.058
Ash	3.94	3.90	3.99	3.87	3.96	0.057	0.718	0.814	0.979
PPV[2]	82.26[a]	89.67[b]	97.89[c]	91.31[b]	80.61[a]	3.644	0.049	0.015	0.208
LPV[3]	194.62[a]	236.18[b]	240.96[b]	224.37[b]	203.10[a]	5.093	0.001	<0.001	0.867
APV[4]	74.54[a]	74.32[a]	85.19[b]	76.46[a]	73.14[a]	1.775	0.008	0.014	0.095

PPV = protein production value; LPV = lipid production value; APV = ash production value.
[a, b, c] Different superscript letterswithin a row indicate significant differences ($P < 0.05$).
[1] HFD+GA 0.5, HFD diet supplemented with 0.5 mg/kg GA; HFD+GA 1.0, HFD diet supplemented with 1.0 mg/kg GA; HFD+GA 1.5, HFD diet supplemented with 1.5 mg/kg GA. Values are mean ± SE of three replicate groups, with 6 fish per tank.
[2] Protein production value (%) = 100 × body protein gain weight/protein intake.
[3] Lipid production value (%) = 100 × body fat gain weigh/fat intake.
[4] Ash production value (%) = 100 × body ash gain weight/ash intake.

other three groups, the expression of lipid production value (LPV) was higher in the HFD and HFD + GA 0.5 groups ($P = 0.001$).

3.3. Intestinal morphology

Intestinal morphology is illustrated in Fig. 1. A significant change was observed in the color of the intestinal tissues in the GA-treated fish. The intestines of the control group had a tan appearance while those of the HFD group were red. Glycyrrhetinic acid treatment mitigated the red color (Fig. 1A).

Intestinal morphological alterations were mitigated by GA treatment. In Fig. 1B, we observed that the intestinal tissues of fish in the HFD group exhibited damage, with the height of the intestinal folds being significantly lower in the HFD-fed fish compared to the other groups ($P < 0.05$). However, the mucosal thickness, intestinal fold width and width of duplicature of fish intestinal tissue were not significantly affected by the diets of different treatment groups ($P > 0.05$). Disturbances in the intestinal villi occurred in the HFD group, including intestinal villus atrophy, intestinal villus adhesion, and intestinal villus shedding. Adding GA to the HFD effectively alleviated intestinal injury (Fig. 1B–C).

Ultrastructural changes of intestinal epithelial cells in the control, HFD and HFD + GA 1.0 groups were observed by transmission electron microscopy analysis. There were no discernible differences between the control group and HFD + GA1.0 group in the structure, which had an intact membrane, tight junctions, and normal mitochondrial morphology (Fig. 1D). However, the HFD group exhibited the accumulation of intestinal epithelial cell pyroptosis, tight junction disrupts, and mitochondrial vacuolation. The intestinal damage in the GA group was considerably alleviated compared to the HFD group.

3.4. Intestinal mitochondrial injury

Fig. 2Adisplays the intestinal ATP and MDA contents of largemouth bass. Adenosine triphosphate content in the intestine of fish fed HFD were significantly decreased in comparison to the control group ($P < 0.05$), and the addition of GA to the HFD significantly increased it ($P < 0.05$). The MDA content in fish fed HFD was significantly higher compared to the control group ($P < 0.05$), but the addition of GA to the HFD group significantly alleviated this phenomenon ($P < 0.05$). Mitochondrial membrane potential (MMP) content was lower in the HFD group compared to the control group. However, it increased with the addition of GA at 1.0 and 1.5 mg/kg. There was no difference between the HFD and HFD + GA 0.5 groups (Fig. 2 B). Similar to the MMP results, the content of ROS was detected using a fluorescence spectrophotometer. Compared with the control group, feeding HFD significantly increased ROS production ($P < 0.05$) (Fig.2C).

3.5. Expression of tight junction-related parameters

In Fig. 3, the parameters related to the tight junction of the fish intestine are presented. The mRNA expression of *ZO-1*, occludin and claudin-1 was significantly lower in the HFD group compared to the control group ($P < 0.05$). The addition of GA to HFD at all three levels significantly elevated the mRNA expression of claudin-1 ($P < 0.05$), but occludin and ZO-1 expression remained largely unchanged by the addition of GA 1.5 mg/kg to HFD (Fig. 3). As illustrated in Fig. 3B, the protein levels of ZO-1, occludin and claudin-1 were significantly lower in the HFD group compared to the control group, but different in the HFD + GA 1.5 group ($P < 0.05$). However, the levels of ZO-1 and claudin-1 were lower in the HFD + GA1.5 group compared to the HFD + GA 1.0 group ($P > 0.05$). For the immunolabeling of ZO-1, intestinal sections from 6 animals were used from each group, and sections from control group without primary antibodies showed no immunolabeling. The staining of ZO-1 was weaker in control group than the other four groups. With the addition of GA, the staining of ZO-1 increased in the HFD + GA 1.0 group as compared to the HFD + GA 0.5 group, while the staining of the HFD + GA 0.5 group decreased to a level similar to the control group. In conclusion, apical staining of ZO-1 was observed in enterocytes in all the observed images (Fig. 3C).

3.6. Intestinal pyroptosis

Figure 4 Ashows the effect of different dietary treatments on the expression of genes related to the pyroptosis pathway in the gut of largemouth bass. The mRNA expression of *caspase-1*, interleukin-1 beta (*IL-1β*), and interleukin-18 (*IL-18*) were significantly higher in the intestines of fish fed HFD as compared to those fed the control diet. Dietary supplementation of GA in HFD at all three levels significantly decreased the mRNA expression of caspase-1, *IL-1β*, *IL-18* compared to the HFD group with no GA ($P < 0.05$).

The protein levels of total HMGB1 were higher in fish fed HFD diets than those fed HFD diets supplemented with GA at 1.0 and 1.5 mg/kg ($P < 0.05$). The cytoplasmic protein expression of HMGB1 was higher in the group fed HFD compared to control group. The addition of GA at all three levels significantly reduced the expression of HMGB1 compared to the HFD group without GA ($P < 0.05$) (Fig. 4B). RAGE, as a receptor for HMGB1, showed significantly higher protein levels in the HFD group as compared to other groups (Fig. 4C) ($P < 0.05$).

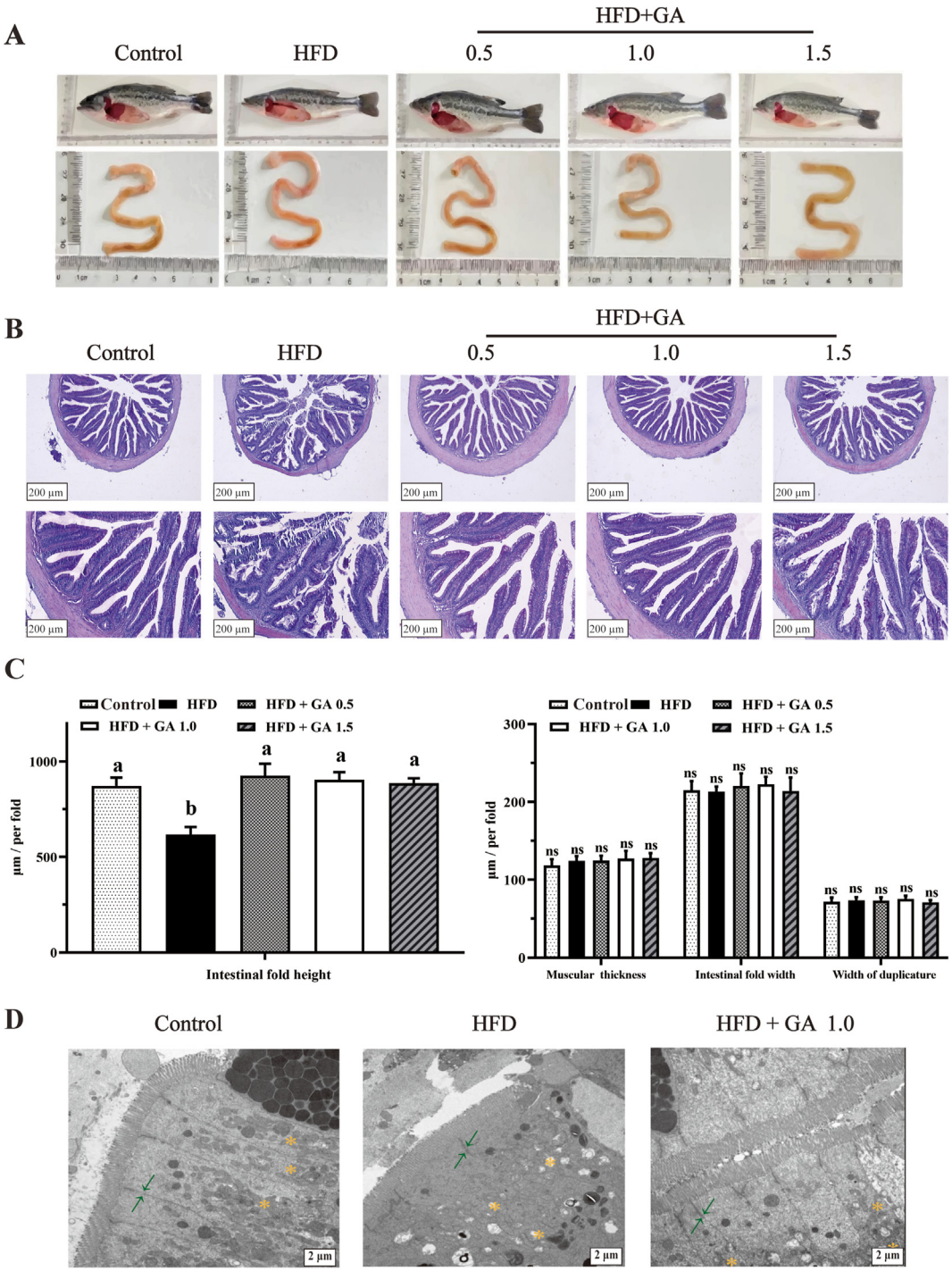

Fig. 1. Glycyrrhetinic acid (GA) alleviates intestinal injury in largemouth bass induced by a high-fat diet (HFD). (A) The pictures of fish body and intestine. (B) Intestine histopathological analysis of largemouth bass. (C) The statistical analysis was performed on the intestinal fold height, intestinal fold width, muscular thickness, and width of duplicature. (D) Transmission electron microscope images of intestines of largemouth bass. The green arrows indicate the intestinal tight junction, and the orange star indicates mitochondrial damage (scale bar = 2 μm). The results are presented as mean ± SE of six replicates. Mean values with different letters indicate significant differences ($P < 0.05$), whereas those with the same letter or no letter indicate no significant differences. ns = no significant differences.

We examined the changes in the expression of key proteins in the pyroptosis signaling pathway using Western blot and found that the protein levels of NLRP3, ASC, GSDME and N-terminal domain of GSDME (GSDME-N) were significantly higher in the HFD group compared to the control group ($P < 0.05$). However, 0.5 and 1.0 mg/kg GA in the HFD group significantly downregulated the protein levels compared to the HFD group ($P < 0.05$). Nevertheless, a high GA dose increased the protein levels compared to other groups that added GA to HFD for NRLP3 but not significant for ASC (Fig. 4C). As demonstrated in Fig. 4D, HFD considerably increased

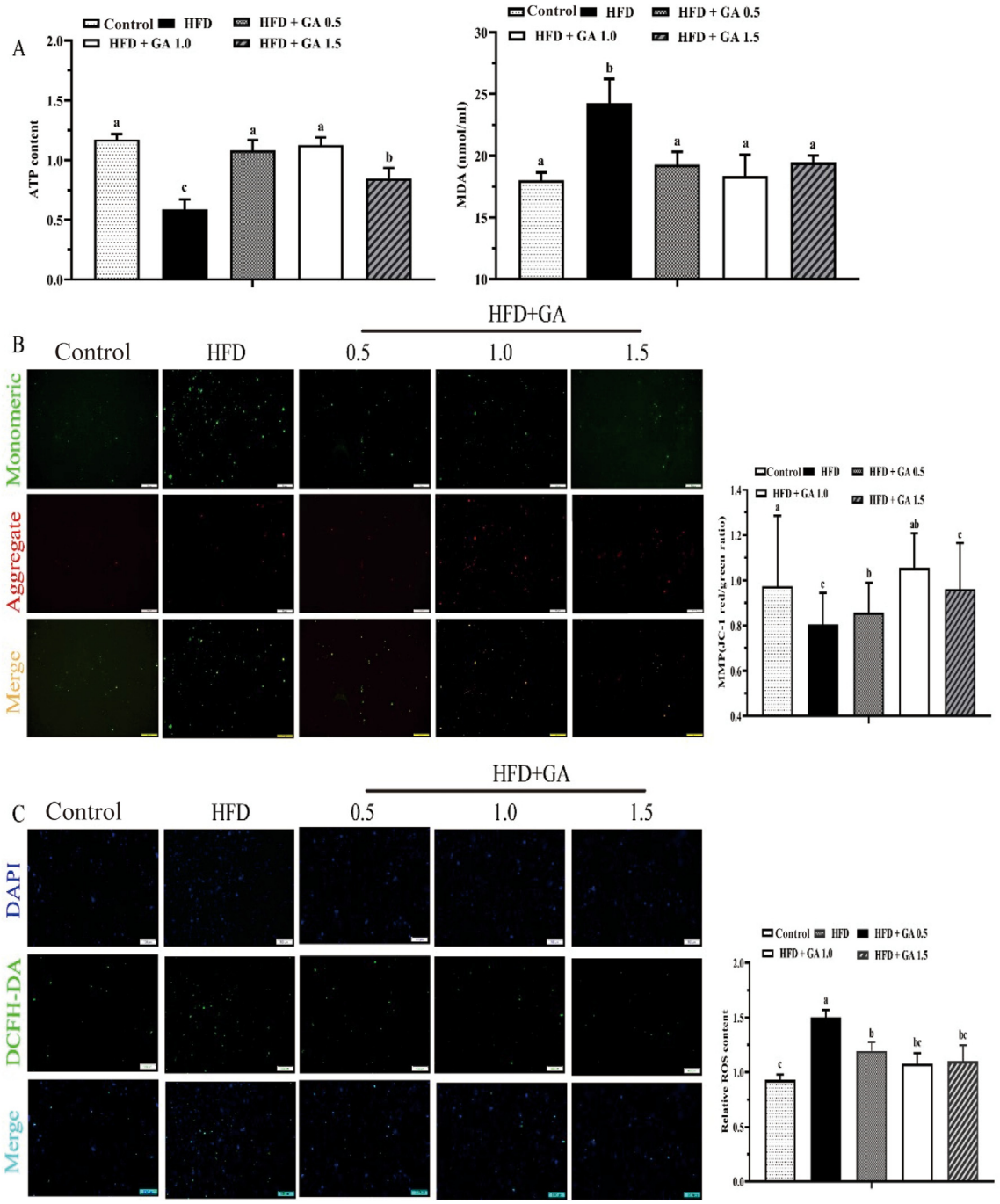

Fig. 2. Glycyrrhetinic acid (GA) alleviates mitochondrial damage in the intestine of largemouth bass induced by a high-fat diet (HFD). (A) The contents of adenosine triphosphate (ATP) and malondialdehyde (MDA) content. (B) The mitochondrial membrane potential (MMP) by JC-1 staining with a fluorescence microscope (scale bar = 100 μm) and detected fluorescence intensities. (C) The intestinal cell suspension was double-stained with 4′,6-diamidino-2′-phenylindole (DAPI) and 2,7-dichlorodihydrofluorescein diacetate (DCFH-DA), and the fluorescence intensities and morphology change were observed under a fluorescence microscope (scale bar = 100 μm), and relative reactive oxygen species (ROS) contents were shown. Bars with different letters indicate a significant difference ($P < 0.05$).

the protein levels of high mobility group box1 (HMGB1) and caspase-1 in the intestine through immunohistochemistry (IHC). Additionally, dietary GA supplementation considerably decreased the expression of HMGB1 and caspase-1 compared to HFD without GA (Fig. 4D). Pyroptosis eventually leads to cell lysis and death, and LDH levels in the serum of largemouth bass fed HFD were significantly higher compared to other groups ($P < 0.05$) (Fig. 4E).

4. Discussion

4.1. GA alleviates reduction in growth performance of largemouth bass caused by HFD

Lipids play a crucial role in growth performance, body composition and energy supplementation. Numerous studies have

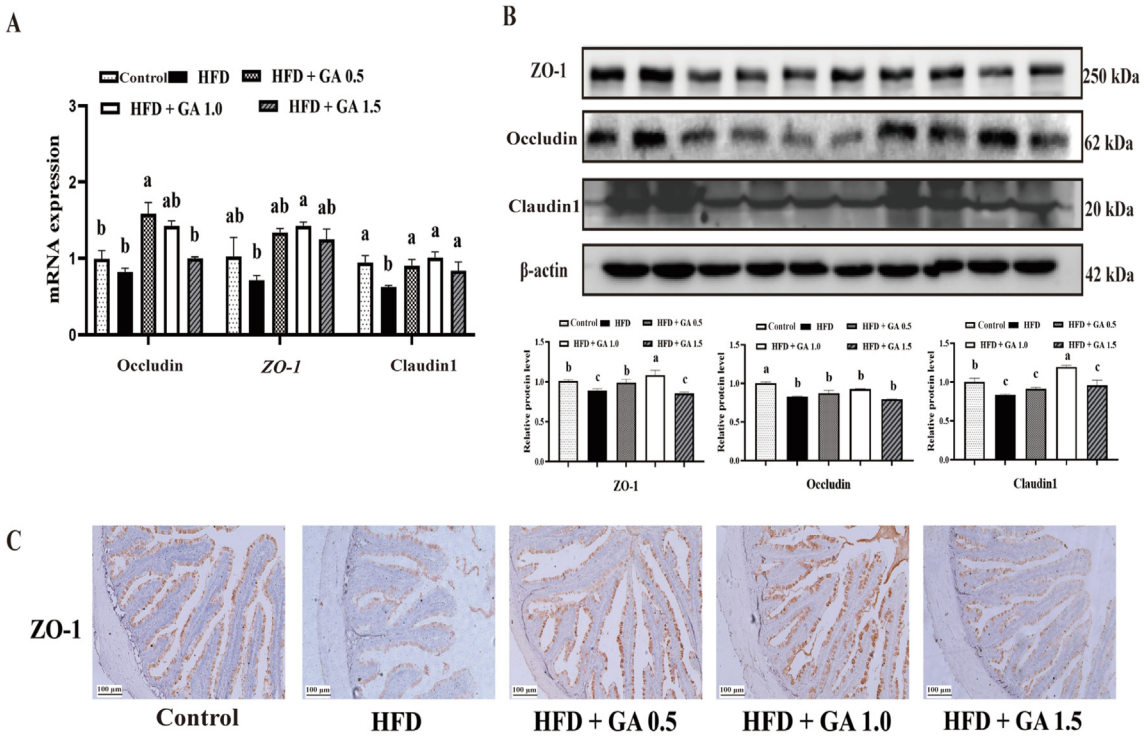

Fig. 3. Intestinal tight junction-related gene expression in largemouth bass fed diets with graded glycyrrhetinic acid (GA) levels for 11 weeks. (A) Zonula occluden-1 (*ZO-1*), occludin, claudin-1-related mRNA levels expression. (B) The levels of related proteins ZO-1, occludin, and claudin-1. (C) Immunohistochemistry for ZO-1 observed under a fluorescence microscope (scale bar = 100 μm). Bars with different letters indicate a significant difference ($P < 0.05$).

demonstrated that fish growth performance and health can be adversely affected by high levels of ROS, oxidative stress and inflammation resulting from the chronic consumption of HFD (Du et al., 2006; Xie et al., 2020). This study illustrates that HFD negatively affect the growth performance of largemouth bass. Some studies have reported an imbalance in energy-to-crude protein ratio when excess fat is added to the diet and can lead to reduced feed consumption and decreased nutrient utilization (Ding et al., 2020). In this study, largemouth bass in the HFD group exhibited reduced FI compared to the control group. Similar results have been observed in blunt snout bream (*Megalobrama amblycephal*) (Jiang et al., 2018) and Nile tilapia (*Oreochromis niloticus*) (Zhang et al., 2020). The suppressed growth performance was further evident in intestinal histology. In the present study, the HFD group had a lower intestinal fold height than the other groups. A previous study suggested that a reduction in the nutrient absorption surface area of the intestine could negatively impact nutrient absorption in fish (Xu et al., 2022).

This study demonstrated that GA supplementation has an effect on the growth performance of largemouth bass, which is consistent with the studies on blunt snout bream (Jiang et al., 2018) and channel catfish (*Ictalurus punctatus*) (Desouky et al., 2020). It is worth noting that fish fed HFD + GA 0.5 and HFD + GA 1.0 exhibited higher FBW and FI compared to the HFD group. Additionally, adding GA increased the intestinal fold height, resulting in an increased intestinal surface area. These results suggest that the addition of GA to HFD can mitigate the adverse effects of HFD on fish growth performance. Glycyrrhetinic acid has been reported to improve growth in blunt snout bream (Jiang et al., 2018), channel catfish (Desouky et al., 2020), and mice (Chen et al., 2017) in previous studies.

Visceral somatic index is an important index that affects the production and commercial value of fish (Wang et al., 2019). Previous studies have shown a corresponding increase in VSI in largemouth bass fed HFD (Guo et al., 2019; Xie et al., 2020). Typically, VSI is influenced by the dietary fat level (Han et al., 2014). Excess fat in the gut and other tissues of fish can accumulate due to a HFD, eventually leading to inflammation (Zhang et al., 2020). The addition of GA had a significant effect on VSI and IW compared to the HFD group without GA (Jiang et al., 2018). The reason for the increase in IW may be attributed to the expanded intestinal absorption area and increased nutrient absorption. The present study indicated that GA may have a significant influence on the lipid metabolism of these tissues. This result is consistent with previous studies in blunt-nosed sea bream (Jiang et al., 2018). Furthermore, consistent with the results of previous studies, feeding a HFD would lead to an increase in lipid metabolism in largemouth bass (Yin et al., 2021). In the present study, the addition of GA had an effect on lipid metabolism in largemouth bass. Our results differ from those of the blunt snout bream (Jiang et al., 2018). Meanwhile, the HFD decreased the moisture content of largemouth bass, while adding GA had no effect compared to the normal group. A similar result was found in largemouth bass (Xie et al., 2020). The differences in results could be attributed to variations in species and feed formulations.

4.2. GA alleviates intestinal pyroptosis of largemouth bass induced by HFD

This study demonstrated the presence of pyroptosis in intestinal injury caused by a HFD, and GA alleviated the pyroptosis by interacting with HMGB1. The NLRP3 inflammasome, which comprises NLRP3, caspase-1, and ASC, is associated with endogenous hazard signals and microbe recognition (Stutz et al., 2017). Inflammasome-triggered pyroptosis is a canonical process mediated by caspase-1. The pore-forming effector protein GSDME is cleaved by caspase to

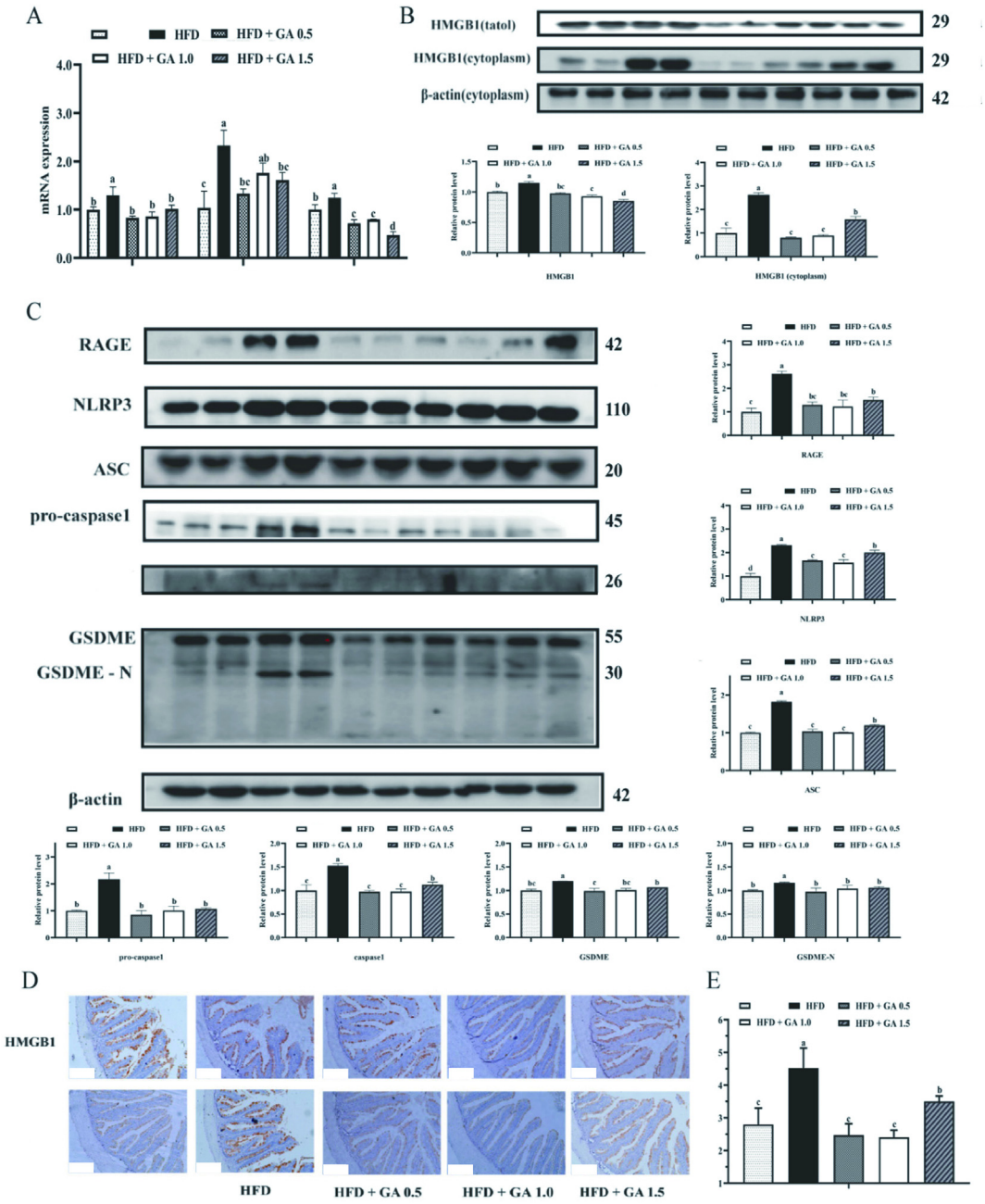

Fig. 4. Effects of glycyrrhetinic acid (GA) on intestinal pyroptosis-related genes expression induced by high fat diets (HFD). (A) The mRNA expression of intestinal pyroptosis-related genes including cysteinyl aspartate specific proteinase 1 (caspase-1), interleukin-1β (*IL-1β*), interleukin-18 (*IL-18*). (B) Protein levels of total HMGB1 and cytoplasm HMGB1. HMGB1 = high mobility group box1. (C) Related protein levels of intestinal pyroptosis-related genes, including RAGE, NLRP3, ASC, pro-caspase-1, caspase-1, GSDME, GSDME-N. RAGE = receptor for advanced glycation end products; NLRP3 = NOD-like receptor family and pyrin domain contain 3; ASC = apoptosis-associated speck-like protein containing a C-terminal caspase recruitment domain; caspase-1 = cysteinyl aspartate specific proteinase 1; GSDME = gasdermin E; GSDME-N=N-terminal domain of GSDME. (D) Immunohistochemistry for caspase-1 observed under a fluorescence microscope (scale bar = 100 μm). (E) Lactate dehydrogenase (LDH) content in the serum. Bars with different letters indicate a significant difference ($P < 0.05$).

release its N-terminal fragment, leading to pyroptosis (Zhou and Fang, 2019).

Glycyrrhetinic acid is one of the primary bioactive components of licorice, and it is widely used in traditional Chinese medicine due to its hepatoprotective, immunomodulatory, anti-inflammatory, and antiviral properties. In the current study, the increased mRNA levels of *NLRP3*, *ASC*, *caspase-1*, *IL-1β*, *IL-18*, and *GSDME* in large-mouth bass fed a HFD indicate the activation of the NLRP3 inflammasome and the subsequent caspase-1-dependent pyroptosis signaling pathway. In addition, GA supplementation in HFD inhibited the upregulation of *NLRP3*, *ASC*, *caspase-1*, *IL-1β*, *IL-18* and *GSDME*. Likewise, pyroptosis-related genes were upregulated in HFD group in terms of protein levels. On the other hand, GA supplementation inhibited the expression of pyroptosis-related genes. This study demonstrated that GA can effectively ameliorate acute intestinal inflammation induced by HFD by inhibiting NLRP3 inflammasome-dependent pyroptosis. These results are in line with previous research conducted in rats, which suggested that pyroptosis induced by HFD is primarily caused by GSDME pore formation (Zhang et al., 2021), unlike mammalian pyroptosis induced by

GSDMD (Li et al., 2020; Wang et al., 2020; Zhang et al., 2021). The present study adds to the evidence that largemouth bass undergoes pyroptosis through GSDME. Caspase-1 mediates pyroptosis triggered by inflammatory vesicles. The similarity in the expression patterns of both *GSDME* and *caspase-1* is intriguing and is also clearly shown in the principal component analysis (PCA) plot representing measured variables in the intestine where they group together. This suggests that NLRP3 may control the expression of these two genes or that they act together. The immunohistochemistry of caspase-1 showed the same trend as protein levels. Pyroptosis is an inflammatory form of programmed cell death accompanied by increased LDH in serum and intestines. Some of the results are consistent with those reported in previous studies (Wu et al., 2022; Zhang et al., 2021), suggesting that GA could also ameliorate HFD-induced acute intestinal inflammation.

4.3. Glycyrrhetinic acid alleviates intestinal barrier damage of largemouth bass caused by HFD

Increasing evidence from human and animal studies suggests that consumption of HFD results in intestinal inflammatory response and intestinal barrier damage (Malesza et al., 2021). The tight intercellular junctions (TJ) in vertebrates are closely related to the physical barrier function of the intestine, and TJ are composed of transmembrane proteins (Wu et al., 2022). Tight intercellular junction protein not only maintains the physical barrier function of fish but also limits the permeability of the intestinal barrier and protects its stability (Suzuki, 2020). Claudin-1, ZO-1, and occludin play a significant role in intestinal barrier integrity, although they are present in low amount in the intestine (Wang et al., 2019). The expression of claudin-1, ZO-1 and occludin mRNA in the intestine of largemouth bass was significantly inhibited by HFD. These results confirm that the TJ component is disrupted by an excess of lipids in the feed. This is supported by the ultrastructural observation of the intestinal apparatus. Similar results have been reported in previous studies, suggesting that HFD impairs the intestinal tight junction in grass carp (*Ctenopharyngodon Idella*) (Liu et al., 2022), tilapia (*O. niloticus*) (Limbu et al., 2019) and mouse (Thomas et al., 2022), and the intestine is more severely affected. Furthermore, adding GA at doses of 0.5 and 1.0 mg/kg showed a protective effect against intestinal barrier damage. The results demonstrated that a certain dose of GA can alleviate and protect the intestine. This effect might be due to the prevention of intestinal barrier function damage caused by pyroptosis, as confirmed by the ultrastructural observation of the intestinal apparatus (Zhang et al., 2022). A similar result suggests that pyroptosis-induced small intestinal macrophage pyrosis caused by HFD can lead to intestinal barrier damage (Ye et al., 2022). The results presented in this study also support the idea that GA can relieve intestinal barrier damage caused by pyroptosis.

4.4. High-fat diets increased ROS and HMGB1 release, leading to pyroptosis

HMGB1 is increasingly recognized as the prototypic alarmin (Yang et al., 2007), and has been implicated in the inflammatory process by binding to its cognate receptor RAGE, ultimately triggering the activation of the NLRP3 (Geng et al., 2015). Previous studies have suggested that HMGB1 is secreted under different conditions via a ROS-dependent mechanism (Min et al., 2017; Tsung et al., 2007), which aligns with the finding that a HFD promotes ROS production. Previous studies have demonstrated that ROS production causes mitochondrial damage, inflammatory responses, and apoptosis in both fish and mammals as a result of HFD treatment. To further investigate the reasons for the increase in ROS, we assessed the extent of mitochondrial damage. Using the JC-1 assay, we observed that the HFD group experienced a loss of mitochondrial membrane potential, which is associated with increased ROS production by mitochondria. Previous studies have also reported that ROS production cause mitochondrial damage (Dang et al., 2022; Easson et al., 2022). On the other hand, we detected the key enzymes related to mitochondrial damage, including MDA and ATP. MDA is a product of lipid peroxidation and is recognized as an important marker of oxidative stress. In this study, the MDA content in largemouth bass tissues significantly increased in response to HFD, while ATP showed the opposite trend. Glycyrrhetinic acid is also known as an antioxidant, capable of reducing ROS production and enhancing the body's antioxidant capacity. Supplementation with GA at 0.5 and 1.0 mg/kg could alleviate mitochondrial damage caused by HFD. In a previous study, GA was found to inhibit ROS production in gastric cancer SGC-7901 cells (Cai et al., 2018). This study further supports the idea that GA can alleviate ROS production in the intestine of largemouth bass, potentially by mitigating mitochondrial damage caused by HFD.

When mitochondria become dysfunctional, excess ROS are produced (Otsuka and Matsui, 2023). A loss of membrane potential in fish fed HFD is apparent due to the lower formation of J-aggregates when JC-1 enters the mitochondria relative to cationic JC-1 monomers. Moreover, higher formation of J-aggregates due to the addition of GA can also disrupt mitochondria. Mitochondria-derived ROS increased in HFD, while the addition of 0.5 and 1.0 mg/kg GA resulted in a decrease in ROS production.

4.5. Excessive GA caused harm to fish body

Glycyrrhetinic acid is a key bioactive compound in licorice, known for its diverse biological and pharmacological activities including anti-inflammatory, antiviral, antioxidant properties (Zhang and Semple-Rowland, 2005). The study demonstrates that GA supplementation can enhance anti-inflammatory capability and positively impact the intestinal barrier of largemouth bass fed on HFD. Glycyrrhetinic acid was found to mitigate proinflammatory responses and reduce ROS production by down-regulating the expression of related genes. In addition, previous studies have suggested that GA interferes with antibody recognition of HMGB1, indicating direct binding to the protein and inhibition of HMGB1 expression (Cavone et al., 2011; Yamaguchi et al., 2012). This aligns with our findings that appropriate dietary supplementation of GA can alleviate intestinal inflammation and damage to the intestinal barrier caused by a HFD. However, we observed that excessive GA supplementation can lead to increased intestinal injury. Some studies have indicated that excessive GA can be cytotoxic, causing cell damage by increasing the release of LDH in human Caco-2 cells (Malekinejad et al., 2022). It is worth noting that GA is a derivative of glycyrrhiza, and excessive glycyrrhiza consumption can result in hypokalemia (Zhang et al., 1994). The mechanism of the effect of excessive GA intake on intestinal health needs further study.

5. Conclusion

In conclusion, HFD can negatively impact the intestinal health of largemouth bass by upregulating the expression of pyroptosis genes and downregulating the expression of tight junction genes in the intestine. Nevertheless, dietary supplementation with GA can enhance the growth performance of largemouth bass and mitigate the adverse effects caused by the HFD. Glycyrrhetinic acid achieves this by boosting anti-inflammatory properties and fortifying intestinal barrier protection functions. Based on the growth performance of largemouth bass fed HFD, the optimal supplemental

levels of GA are 0.5 and 1.0 mg/kg and the ideal supplemental level of GA is 1.0 mg/kg as it effectively enhances anti-inflammatory properties and tight junction structure.

CRediT author statement

Quanquan Cao: Formal analysis, Investigation, Methodology, Visualization, Writing – original draft. **Zhihao Zhang:** Formal analysis, Investigation, Methodology, Visualization, Writing – original draft. **Ju Zhao:** Investigation, Software, Visualization. **Lin Feng:** Investigation. **Weidan Jiang:** Investigation. **Pei Wu:** Investigation. **Juan Zhao:** Investigation. **Haifeng Liu:** Conceptualization, Methodology, Resources, Supervision, Validation, Visualization, Writing – review & editing. **Jun Jiang:** Conceptualization, Methodology, Resources, Supervision, Validation, Visualization, Writing – review & editing.

Declaration of competing interest

We declare that we have no financial and personal relationships with other people or organizations that can inappropriately influence our work, and there is no professional or other personal interest of any nature or kind in any product, service and/or company that could be construed as influencing the content of this paper.

Acknowledgements

This research was funded by the National Natural Science Foundation of China (32172987), National Key R&D Program of China (2019YFD0900200) and Yucheng District (Ya'an City) cooperating with Sichuan Agricultural University project (2023QXHZ03).

References

AOAC. Official methods of analysis. 15th ed. Arlington, VA: Assoc. Off. Anal. Chem.; 1990.

Arab HH, Al-Shorbagy MY, Saad MA. Activation of autophagy and suppression of apoptosis by dapagliflozin attenuates experimental inflammatory bowel disease in rats: targeting AMPK/mTOR, HMGB1/RAGE and Nrf 2/HO-1 pathways. Chem Biol Interact 2021;335:109368. https://doi.org/10.1016/j.cbi.2021.109368.

Bahnasa M. Effect of dietary protein levels on growth performance and body composition of monosex Nile Tilapia, *Oreochromis niloticus L.* Reared in fertilized tanks. Pakistan J Nutr 2009;8(5):674–8. https://doi.org/10.3923/pjn.2009.674.678.

Bianchi ME, Crippa MP, Manfredi AA, Mezzapelle R, Rovere QP, Venereau E. High-mobility group box 1 protein orchestrates responses to tissue damage via inflammation, innate and adaptive immunity, and tissue repair. Immunol Rev 2017;280(1):74–82. https://doi.org/10.1111/imr.12601.

Buzete GM, Rocha RT, Estevan MS, Oba YE, Uribe GL, Franceschini VI, et al. Heart structure in the amazonian teleost Arapaima gigas (*osteoglossiformes, arapaimidae*). J Anat 2019;234(3):327–37. https://doi.org/10.1111/joa.12919.

Cai H, Chen X, Zhang J, Wang J. 18β-glycyrrhetinic acid inhibits migration and invasion of human gastric cancer cells via the ROS/PKC-alpha/ERK pathway. J Nat Med 2018;72(1):252–9. https://doi.org/10.1007/s11418-017-1145-y.

Cavone L, Muzzi M, Mencucci R, Sparatore B, Pedrazzi M, Moroni F, et al. 18beta-glycyrrhetic acid inhibits immune activation triggered by HMGB1, a pro-inflammatory protein found in the tear fluid during conjunctivitis and blepharitis. Ocul Immunol Inflamm 2011;19(3):180–5. https://doi.org/10.3109/09273948.2010.538121.

Chatzifotis S, Panagiotidou M, Papaioannou N, Pavlidis M, Nengas I, Mylonas CC. Effect of dietary lipid levels on growth, feed utilization, body composition and serum metabolites of meagre (*Argyrosomus regius*) juveniles. Aquaculture 2010;307(1):65–70. https://doi.org/10.1016/j.aquaculture.2010.07.002.

Chen J, Zhang W, Zhang L, Zhang J, Chen X, Yang M, et al. Glycyrrhetinic acid alleviates radiation-induced lung injury in mice. J Radiat Res 2017;58(1):41–7. https://doi.org/10.1093/jrr/rrw091.

Chen W, Chang K, Chen J, Zhao X, Gao S. Dietary sodium butyrate supplementation attenuates intestinal inflammatory response and improves gut microbiota composition in largemouth bass (*Micropterus salmoides*) fed with a high soybean meal diet. Fish Physiol Biochem 2021;47(6):1805–19. https://doi.org/10.1007/s10695-021-01004-w.

Chen W, Gao S, Chang K, Zhao X, Niu B. Dietary sodium butyrate supplementation improves fish growth, intestinal microbiota composition, and liver health in largemouth bass (*Micropterus salmoides*) fed high-fat diets. Aquaculture 2023;564:739040. https://doi.org/10.1016/j.aquaculture.2022.739040.

Dang D, Meng Z, Zhang C, Li Z, Wei J, Wu H. Heme induces intestinal epithelial cell ferroptosis via mitochondrial dysfunction in transfusion-associated necrotizing enterocolitis. Faseb J 2022;36(12):e22649. https://doi.org/10.1096/fj.202200853RRR.

De Sliva, Sena S, Gunasekera, Rasanthi M, Shim KF. Interactions of varying dietary protein and lipid leveks in young red tilapia (*Oreochromis mossambicus*): evidence of protein sparing. Aquaculture 1991;3:95. https://doi.org/10.1016/0044-8486(91)90096-P.

Desouky HE, Jiang GZ, Zhang DD, Abasubong KP, Yuan X, Li XF, et al. Influences of glycyrrhetinic acid (GA) dietary supplementation on growth, feed utilization, and expression of lipid metabolism genes in channel catfish (*Ictalurus punctatus*) fed a high-fat diet. Fish Physiol Biochem 2020;46(2):653–63. https://doi.org/10.1007/s10695-019-00740-4.

Ding T, Xu N, Liu Y, Du J, Xiang X, Xu D, et al. Effect of dietary bile acid (BA) on the growth performance, body composition, antioxidant responses and expression of lipid metabolism-related genes of juvenile large yellow croaker (*Larimichthys crocea*) fed high-lipid diets. Aquaculture 2020;518:734768.

Du ZY, Clouet P, Zheng WH, Degrace P, Tian LX, Liu YJ. Biochemical hepatic alterations and body lipid composition in the herbivorous grass carp (*Ctenopharyngodon idella*) fed high-fat diets. Br J Nutr 2006;95(5):905–15. https://doi.org/10.1079/bjn20061733.

Easson S, Singh RD, Connors L, Scheidl T, Baker L, Jadli A, et al. Exploring oxidative stress and endothelial dysfunction as a mechanism linking bisphenol S exposure to vascular disease in human umbilical vein endothelial cells and a mouse model of postnatal exposure. Environ Int 2022;170:107603. https://doi.org/10.1016/j.envint.2022.107603.

Fiore C, Eisenhut M, Krausse R, Ragazzi E, Pellati D, Armanini D, et al. Antiviral effects of Glycyrrhiza species. Phytother Res 2008;22(2):141–8. https://doi.org/10.1002/ptr.2295.

Franchi L, Eigenbrod T, Munoz-Planillo R, Nunez G. The inflammasome: a caspase-1-activation platform that regulates immune responses and disease pathogenesis. Nat Immunol 2009;10(3):241–7. https://doi.org/10.1038/ni.1703.

Gaul S, Leszczynska A, Alegre F, Kaufmann B, Johnson CD, Adams LA, et al. Hepatocyte pyroptosis and release of inflammasome particles induce stellate cell activation and liver fibrosis. J Hepatol 2021;74(1):156–67. https://doi.org/10.1016/j.jhep.2020.07.041.

Geng Y, Ma Q, Liu YN, Peng N, Yuan FF, Li XG, et al. Heatstroke induces liver injury via IL-1β and HMGB1-induced pyroptosis. J Hepatol 2015;63(3):622–33. https://doi.org/10.1016/j.jhep.2015.04.010.

Guo J, Zhou Y, Zhao H, Chen W, Chen Y, Lin S. Effect of dietary lipid level on growth, lipid metabolism and oxidative status of largemouth bass, *Micropterus salmoides*. Aquaculture 2019;506:394–400. https://doi.org/10.1016/j.aquaculture.2019.04.007.

Han T, Li X, Wang J, Hu S, Jiang Y, Zhong X. Effect of dietary lipid level on growth, feed utilization and body composition of juvenile giant croaker *Nibea japonica*. Aquaculture 2014;434:145–50. https://doi.org/10.1016/j.aquaculture.2014.08.012.

Han SJ, Min HJ, Yoon SC, Ko EA, Park SJ, Yoon JH, et al. HMGB1 in the pathogenesis of ultraviolet-induced ocular surface inflammation. Cell Death Dis 2015;6(8):e1863. https://doi.org/10.1038/cddis.2015.199.

Hillestad M, Johnsen F. High-energy/low-protein diets for Atlantic salmon: effects on growth, nutrient retention and slaughter quality. Aquaculture 1994;124(1):109–16.

Huo H, Wang S, Bai Y, Liao J, Li X, Zhang H, et al. Copper exposure induces mitochondrial dynamic disorder and oxidative stress via mitochondrial unfolded protein response in pig fundic gland. Ecotoxicol Environ Saf 2021;223:112587.

Jia C, Zhang J, Chen H, Zhuge Y, Chen H, Qian F, et al. Endothelial cell pyroptosis plays an important role in Kawasaki disease via HMGB1/RAGE/cathespin B signaling pathway and NLRP3 inflammasome activation. Cell Death Dis 2019;10(10):778. https://doi.org/10.1038/s41419-019-2021-3.

Jiang GZ, Zhou M, Zhang DD, Li XF, Liu WB. The mechanism of action of a fat regulator: glycyrrhetinic acid (GA) stimulating fatty acid transmembrane and intracellular transport in blunt snout bream (*Megalobrama amblycephala*). Comp Biochem Physiol Mol Integr Physiol 2018;226:83–90. https://doi.org/10.1016/j.cbpa.2018.08.014.

Kersse K, Lamkanfi M, Bertrand M, Vanden BT, Vandenabeele P. Interaction patches of procaspase-1 caspase recruitment domains (cards) are differently involved in procaspase-1 activation and receptor-interacting protein 2 (RIP2)-dependent nuclear factor kappab signaling. J Biol Chem 2011;286(41):35874–82. https://doi.org/10.1074/jbc.M111.242321.

Li JY, Gao K, Shao T, Fan DD, Hu CB, Sun CC, et al. Characterization of an NLRP1 inflammasome from zebrafish reveals a unique sequential activation mechanism underlying inflammatory caspases in ancient vertebrates. J Immunol 2018;201(7):1946–66. https://doi.org/10.4049/jimmunol.1800498.

Li X, Wei X, Sun Y, Du J, Li X, Xun Z, et al. High-fat diet promotes experimental colitis by inducing oxidative stress in the colon. Am J Physiol Gastrointest Liver Physiol 2019;317(4):G453–62. https://doi.org/10.1152/ajpgi.00103.2019.

Li JY, Wang YY, Shao T, Fan DD, Lin AF, Xiang LX, et al. The zebrafish NLRP3 inflammasome has functional roles in ASC-dependent interleukin-1β maturation and gasdermin E-mediated pyroptosis. J Biol Chem 2020;295(4):1120–41. https://doi.org/10.1074/jbc.RA119.011751.

Limbu SM, Ma Q, Zhang ML, Du ZY. High fat diet worsens the adverse effects of antibiotic on intestinal health in juvenile Nile tilapia (*Oreochromis niloticus*). Sci Total Environ 2019;680:169–80. https://doi.org/10.1016/j.scitotenv.2019.05.067.

Liu F, Wang X, Cui Y, Yin Y, Qiu D, Li S, et al. Apple polyphenols extract (ape) alleviated dextran sulfate sodium induced acute ulcerative colitis and accompanying neuroinflammation via inhibition of apoptosis and pyroptosis. Foods 2021;10(11):2711. https://doi.org/10.3390/foods10112711.
Liu S, Yu H, Li P, Wang C, Liu G, Zhang X, et al. Dietary nano-selenium alleviated intestinal damage of juvenile grass carp (*Ctenopharyngodon idella*) induced by high-fat diet: insight from intestinal morphology, tight junction, inflammation, anti-oxidization and intestinal microbiota. Anim Nutr 2022;8(1):235–48. https://doi.org/10.1016/j.aninu.2021.07.001.
Malekinejad M, Pashaee MR, Malekinejad H. 18β-Glycyrrhetinic acid altered the intestinal permeability in the human Caco-2 monolayer cell model. Eur J Nutr 2022;61(7):3437–47. https://doi.org/10.1007/s00394-022-02900-4.
Malesza IJ, Malesza M, Walkowiak J, Mussin N, Walkowiak D, Aringazina R, et al. High-fat, western-style diet, systemic inflammation, and gut microbiota: a narrative review. Cells 2021;10(11):3164. https://doi.org/10.3390/cells10113164.
Min HJ, Kim JH, Yoo JE, Oh JH, Kim KS, Yoon JH, et al. ROS-dependent HMGB1 secretion upregulates IL-8 in upper airway epithelial cells under hypoxic condition. Mucosal Immunol 2017;10(3):685–94. https://doi.org/10.1038/mi.2016.82.
Mollica L, De Marchis F, Spitaleri A, Dallacosta C, Pennacchini D, Zamai M, et al. Glycyrrhizin binds to high-mobility group box 1 protein and inhibits its cytokine activities. Chem Biol 2007;14(4):431–41. https://doi.org/10.1016/j.chembiol.2007.03.007.
Morais S, Bell JG, Robertson DA, Roy WJ, Morris PC. Protein/lipid ratios in extruded diets for Atlantic cod (*Gadus morhua L.*): effects on growth, feed utilisation, muscle composition and liver histology. Aquaculture 2001;203(1):101–19. https://doi.org/10.1016/S0044-8486(01)00618-4.
Otsuka T, Matsui H. Fish models for exploring mitochondrial dysfunction affecting neurodegenerative disorders. Int J Mol Sci 2023;24(8):7079.
Roman Paduch MK. Antitumor and antiviral activity of pentacyclic triterpenes. Mini-Reviews Org Chem 2014;11:262–8. https://doi.org/10.2174/1570193X1103140915105240.
Sagada G, Chen J, Shen B, Huang A, Sun L, Jiang J, et al. Optimizing protein and lipid levels in practical diet for juvenile northern snakehead fish (*Channa argus*). Anim Nutr 2017;3(2):156–63. https://doi.org/10.1016/j.aninu.2017.03.003.
Shi J, Zhao Y, Wang K, Shi X, Wang Y, Huang H, et al. Cleavage of GSDMD by inflammatory caspases determines pyroptotic cell death. Nature 2015;526(7575):660–5. https://doi.org/10.1038/nature15514.
Sims GP, Rowe DC, Rietdijk ST, Herbst R, Coyle AJ. HMGB1 and RAGE in inflammation and cancer. Annu Rev Immunol 2010;28:367–88. https://doi.org/10.1146/annurev.immunol.021908.132603.
Srinivasula SM, Poyet JL, Razmara M, Datta P, Zhang Z, Alnemri ES. The pyrin-card protein asc is an activating adaptor for caspase-1. J Biol Chem 2002;277(24):21119–22. https://doi.org/10.1074/jbc.C200179200.
Stutz A, Kolbe CC, Stahl R, Horvath GL, Franklin BSVR, Brinkschulte R, et al. NLRP3 inflammasome assembly is regulated by phosphorylation of the pyrin domain. J Exp Med 2017;214(6):1725–36. https://doi.org/10.1084/jem.20160933.
Suzuki T. Regulation of the intestinal barrier by nutrients: the role of tight junctions. Anim Sci J 2020;91(1):e13357. https://doi.org/10.1111/asj.13357.
Thomas SS, Cha YS, Kim KA. Protective effect of perilla oil against dextran sodium sulfate-induced colitis in mice challenged with a high-fat diet. J Med Food 2022;25(11):1021–8. https://doi.org/10.1089/jmf.2022.K.0071.
Tsung A, Klune JR, Zhang X, Jeyabalan G, Cao Z, Peng X, et al. HMGB1 release induced by liver ischemia involves toll-like receptor 4–dependent reactive oxygen species production and calcium-mediated signaling. J Exp Med 2007;204(12):2913–23. https://doi.org/10.1084/jem.20070247.
Wang J, Liu Y, Tian L, Mai K, Du Z, Wang Y, et al. Effect of dietary lipid level on growth performance, lipid deposition, hepatic lipogenesis in juvenile cobia (*Rachycentron canadum*). Aquaculture 2005;249(1):439–47. https://doi.org/10.1016/j.aquaculture.2005.04.038.
Wang J, Zhang C, Guo C, Li X. Chitosan ameliorates dss-induced ulcerative colitis mice by enhancing intestinal barrier function and improving microflora. Int J Mol Sci 2019a;20(22):5751. https://doi.org/10.3390/ijms20225751.
Wang L, Zhang W, Gladstone S, Ng W, Zhang J, Shao Q. Effects of isoenergetic diets with varying protein and lipid levels on the growth, feed utilization, metabolic enzymes activities, antioxidative status and serum biochemical parameters of black sea bream (*Acanthopagrus schlegelii*). Aquaculture 2019b;513:734397. https://doi.org/10.1016/j.aquaculture.2019.734397.
Wang Z, Gu Z, Hou Q, Chen W, Mu D, Zhang Y, et al. Zebrafish gsdmeb cleavage-gated pyroptosis drives septic acute kidney injury in vivo. J Immunol 2020;204(7):1929–42. https://doi.org/10.4049/jimmunol.1901456.
Wang M, Chen Z, Wang Y, Zou J, Li S, Guo X, et al. Largemouth bass (*Micropterus salmoides*) exhibited better growth potential after adaptation to dietary cottonseed protein concentrate inclusion but experienced higher inflammatory risk during bacterial infection. Front Immunol 2022;13:997985. https://doi.org/10.3389/fimmu.2022.997985.
Wei H, Bu R, Yang Q, Jia J, Li T, Wang Q, et al. Exendin-4 protects against hyperglycemia-induced cardiomyocyte pyroptosis via the AMPK-TXNIP pathway. J Diabetes Res 2019;2019:8905917. https://doi.org/10.1155/2019/8905917.
Wu S, Li Z, Ye M, Liu C, Liu H, He X, et al. A specific caspase-1 inhibitor, alleviates lung ischemia reperfusion injury by suppressing endothelial pyroptosis and barrier dysfunction. BioMed Res Int 2021;2021:4525988. https://doi.org/10.1155/2021/4525988.
Wu P, Su Y, Feng L, Jiang W, Kuang S, Tang L, et al. Optimal dl-methionyl-dl-methionine supplementation improved intestinal physical barrier function by changing antioxidant capacity, apoptosis and tight junction proteins in the intestine of juvenile grass carp (*ctenopharyngodon idella*). Antioxidants 2022;11(9). https://doi.org/10.3390/antiox11091652.
Xie S, Yin P, Tian L, Yu Y, Liu Y, Niu J. Dietary supplementation of astaxanthin improved the growth performance, antioxidant ability and immune response of juvenile largemouth bass (*micropterus salmoides*) fed high-fat diet. Mar Drugs 2020;18(12):642. https://doi.org/10.3390/md18120642.
Xu J, Yao X, Lin Y, Chi S, Zhang S, Cao J, et al. Schizochytrium limacinum altered antioxidant capacity and transcriptome profiles in Pacific white shrimp fed a low-fishmeal diet. Aquac Rep 2022;27:101399. https://doi.org/10.1016/j.aqrep.2022.101399.
Yamada M. ATP-dependent chromatin structural modulation by umtiprotein complex including HMGB1. J Biochem 2004;135(1):149–53. https://doi.org/10.1093/jb/mvh017.
Yamaguchi H, Kidachi Y, Kamiie K, Noshita T, Umetsu H. Structural insight into the ligand-receptor interaction between glycyrrhetinic acid (GA) and the high-mobility group protein B1 (HMGB1)-DNA complex. Bioinformation 2012;8(23):1147–53. https://doi.org/10.6026/97320630081147.
Yang D, Chen Q, Yang H, Tracey KJ, Bustin M, Oppenheim JJ. High mobility group box-1 protein induces the migration and activation of human dendritic cells and acts as an alarmin. J Leukoc Biol 2007;81(1):59–66. https://doi.org/10.1189/jlb.0306180.
Ye H, Ma S, Qiu Z, Huang S, Deng G, Li Y, et al. Poria cocos polysaccharides rescue pyroptosis-driven gut vascular barrier disruption in order to alleviates non-alcoholic steatohepatitis. J Ethnopharmacol 2022;296:115457. https://doi.org/10.1016/j.jep.2022.115457.
Yin P, Xie S, Zhuang Z, Fang H, Tian L, Liu Y, et al. Chlorogenic acid improves health in juvenile largemouth bass (*Micropterus salmoides*) fed high-fat diets: involvement of lipid metabolism, antioxidant ability, inflammatory response, and intestinal integrity. Aquaculture 2021;545:737169. https://doi.org/10.1016/j.aquaculture.2021.737169.
Yuan J, Ni M, Liu M, Wang H, Zhang C, Mi G, et al. Analysis of the growth performances, muscle quality, blood biochemistry and antioxidant status of *Micropterus salmo*ides farmed in in-pond raceway systems versus usual-pond systems. Aquaculture 2019;511:734241. https://doi.org/10.1016/j.aquaculture.2019.734241.
Zhang Y, Semple-Rowland SL. Rhythmic expression of clock-controlled genes in retinal photoreceptors is sensitive to 18β-glycyrrhetnic acid and 18α-glycyrrhetnic acid-3-hemisuccinate. Brain Res Mol Brain Res 2005;135(1–2):30–9. https://doi.org/10.1016/j.molbrainres.2004.11.013.
Zhang YD, Lorenzo B, Reidenberg MM. Inhibition of 11 beta-hydroxysteroid dehydrogenase obtained from Guinea pig kidney by furosemide, naringenin and some other compounds. J Steroid Biochem Mol Biol 1994;49(1):81–5. https://doi.org/10.1016/0960-0760(94)90304-2.
Zhang YX, Jiang ZY, Han SL, Li LY, Qiao F, Zhang ML, et al. Inhibition of intestinal lipases alleviates the adverse effects caused by high-fat diet in Nile tilapia. Fish Physiol Biochem 2020;46(1):111–23. https://doi.org/10.1007/s10695-019-00701-x.
Zhang X, Shang X, Jin S, Ma Z, Wang H, Ao N, et al. Vitamin D ameliorates high-fat-diet-induced hepatic injury via inhibiting pyroptosis and alters gut microbiota in rats. Arch Biochem Biophys 2021;705:108894. https://doi.org/10.1016/j.abb.2021.108894.
Zhang Y, Liu Y, Xie Z, Liu Q, Zhuang Y, Xie W, et al. Inhibition of PFKFB preserves intestinal barrier function in sepsis by inhibiting NLRP3/GSDMD. Oxid Med Cell Longev 2022;2022:8704016. https://doi.org/10.1155/2022/8704016.
Zhou CB, Fang JY. The role of pyroptosis in gastrointestinal cancer and immune responses to intestinal microbial infection. Biochim Biophys Acta Rev Cancer 2019;1872(1):1–10. https://doi.org/10.1016/j.bbcan.2019.05.001.